Modeling and Characterization of Dielectric-Charging Effects in RF MEMS Capacitive Switches

Xiaobin Yuan, *Student Member, IEEE,* James C. M. Hwang, *Fellow, IEEE,* David Forehand, *Member, IEEE,* and Charles L. Goldsmith, *Senior Member, IEEE*

***Abstract* — For the first time, charging and discharging of traps in the dielectric of state-of-the-art RF MEMS capacitive switches were characterized in detail. Densities and time constants of different trap species were extracted under different control voltages. It was found that, while charging and discharging time constants are relatively independent of control voltage, steady-state charge densities increase exponentially with control voltage. A simple charge model was constructed to predict the amount of charge injected into the dielectric and the corresponding shift in actuation voltage. Good agreement was obtained between the model prediction and experimental data.**

***Index Terms* — RF, MEMS, switch, dielectric, charging, trap.**

I. Introduction

The commercialization of RF MEMS devices is hindered by a number of factors such as reliability and packaging. In particular, the lifetime of electrostatically actuated RF MEMS capacitive switches can be affected by dielectric-charging effects [1]. The dielectric is typically low-temperature deposited silicon dioxide or nitride with a high density (10^{18} /cm^3) of traps associated with silicon dangling bonds. During switch operation, the electric field across the dielectric can be as high as 10^6 V/cm causing electrons or holes to be injected into the switch dielectric and become trapped. With repeated operation, charge gradually builds up in the dielectric resulting in actuation-voltage shift and/or stiction [2].

Although a general charge model exists in the literature [3], there has been no effort to accurately model the charging state of the dielectric and its impact on actuation voltage. Using a special test structure and setup, we directly characterized charging and discharging currents in state-of-the-art RF MEMS capacitive switches and constructed a simple charge model to predict their effects on the operation of the switches under different control voltages. The model was found to be in good agreement with measured actuation-voltage shift.

Manuscript submitted on November 18, 2004. Work was partially supported by the Air Force Research Laboratory under Contract No. F33615-03-C-7003. The contract was funded by the Defense Advanced Research Projects Area (DARPA) under the Harsh Environment, Robust Micromachined Technology (HERMIT) program.

X. Yuan and J. C. M. Hwang are with Lehigh University, Bethlehem, PA 18015 USA. X. Yuan can be contacted at (610) 758-5109 or xiy2@lehigh.edu.

D. Forehand and C. Goldsmith is with MEMtronics Corp., Plano, TX 75075 USA.

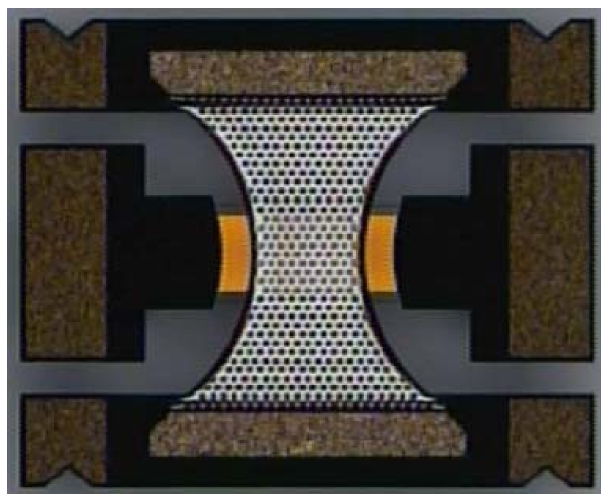

Fig. 1. Top view of a state-of-the-art RF MEMS capacitive switch.

II. Experimental

Fig. 1 illustrates a state-of-the-art metal-dielectric-metal RF MEMS capacitive switch fabricated on a glass substrate. The dielectric is sputtered silicon dioxide with a thickness of 0.25 μm and a dielectric constant of 4.0. The top electrode is a 0.3-μm-thick flexible aluminum membrane that is grounded. The bottom chromium/gold electrode serves as the center conductor of a 50 Ω coplanar waveguide for the RF signal. Without any electrostatic force, the membrane is normally suspended in air 2.5 μm above the dielectric. Control voltage in the range of 25-35 V is applied to the bottom electrode, which brings the membrane in contact with the dielectric thus forming a 120 μm x 80 μm capacitor. The switch has low insertion loss (0.06 dB) and reasonable isolation (15 dB) at 35 GHz. The switching time is less than 10 μs. Details of the design, fabrication and performance of the switches will be reported elsewhere.

0-7803-8846-1/05/$20.00 (C) 2005 IEEE

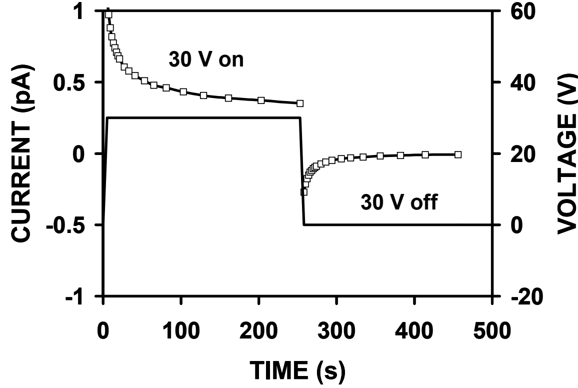

Fig. 2. Measured charging current under 30 V and discharging current after removal of the voltage on an MIM test structure. Solid line is the control voltage waveform.

In order to quantitatively characterize the trap states of the dielectric, charging and discharging current transients [4] were measured on switches whose membrane was intentionally fabricated in a permanently down position (without the sacrificial release layer) thus resembling a metal-insulator-metal capacitor. A precision semiconductor parameter analyzer was used to force a voltage pulse onto the switch while sensing the current transient. Well-guarded probe station and probes were used to suppress the capacitive and leakage currents in the measurement path, thus extending the transient current measurement range below pA level.

As shown in Fig. 2, when a voltage pulse is applied to a permanently down switch, the total current includes displacement current, trap charging current, and steady-state leakage current. After this voltage is removed, charges accumulated on the electrodes and the dielectric begin to discharge. Since the time constant for the displacement current is of the order of milliseconds, the current transients shown in Fig. 2 comprise mainly trap charging and discharging currents. In this case, trap density and charging/discharging time constants can be extracted for different trap species.

III. Measurement Results and Model Extraction

The injected charge density in the dielectric can be modeled as

$$Q = \sum_J Q^J [1 - \exp(-t_{ON} / \tau_C^J)] \exp(-t_{OFF} / \tau_D^J) \qquad (1)$$

where Q^J is the steady-state charge density of the *Jth* species of trap, τ_C and τ_D are the charging and discharging time constants, t_{ON} and t_{OFF} are the on and off times of the switch corresponding to the charging and discharging times.

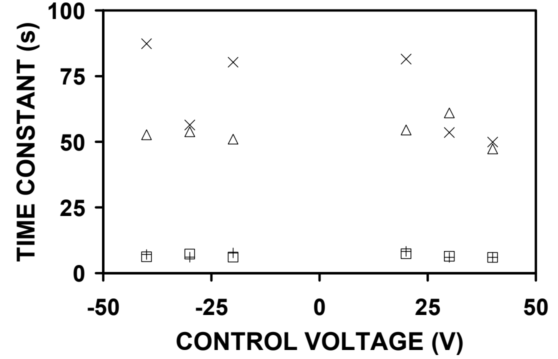

(a)

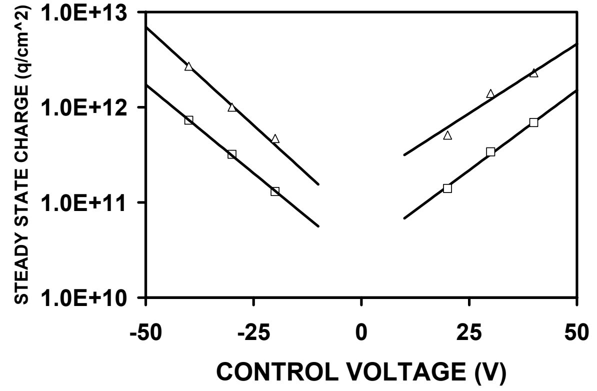

(b)

Fig. 3. (a) Trap 1 (□) charging and (+) discharging and trap 2 (Δ) charging and (x) discharging time constants and (b) (symbols) extracted and (lines) fitted steady-state charge density for (□) trap 1 and (Δ) trap 2 under -40, -30, -20, 20, 30 and 40 V.

Assuming all traps are empty before applying the charging voltage pulse, current transient due to charging of the trap states after the voltage is turned on is

$$I_C = qA \frac{dQ}{dt} = qA \sum_J \frac{Q^J}{\tau_C^J} \exp(-t_{ON} / \tau_C^J) \qquad (2)$$

where q is the electron charge and A is the surface area of the dielectric. Similarly, assuming the traps are all charged during the voltage pulse duration, current transient due to the discharging of the trap states after removal of the voltage is

$$I_D = qA \frac{dQ}{dt} = -qA \sum_J \frac{Q^J}{\tau_D^J} \exp(-t_{OFF} / \tau_D^J) \qquad (3)$$

Switch lifetime has exhibited an exponential dependence on the control voltage [1], implying that either the charge density or the time constant is strongly dependent on voltage. To investigate the voltage dependence of the model parameters, charging and discharging currents were measured on permanently

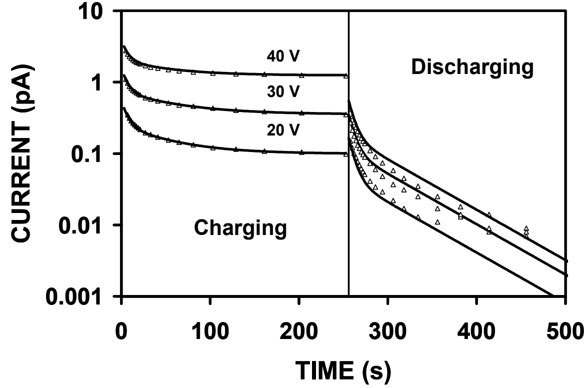

(a)

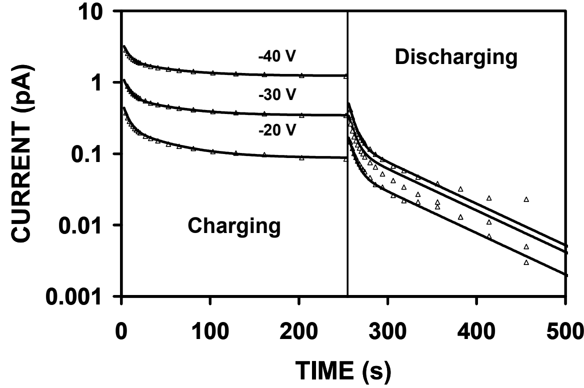

(b)

Fig. 4. Absolute values of (symbols) measured and (lines) calculated charging and discharging current transients under (a) positive and (b) negative control voltages.

TABLE I
EXTRACTED MODEL PARAMETERS

POSITIVE BIAS				
J	τ_C (s)	τ_D (s)	Q_0 (cm^{-2})	V_0 (V)
1	6.6	6.8	3.1×10^{10}	12.9
2	54.3	61.6	1.6×10^{11}	14.9
NEGATIVE BIAS				
J	τ_C (s)	τ_D (s)	Q_0 (cm^{-2})	V_0 (V)
1	6.5	7.0	2.4×10^{10}	11.7
2	52.5	74.7	6.0×10^{10}	10.5

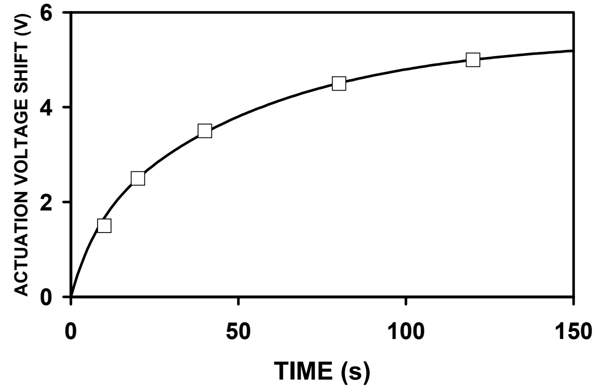

Fig. 5. (□) Measured and (—) modeled actuation-voltage shift after 10, 20, 40, 80 and 120 s of -30 V stress on the switch. The charge sheet is assumed to be 90 nm away from the bottom switch electrode.

down switches under control voltages both above and below the actuation voltage of normal switches. Then the model parameters (Q^J, τ_C and τ_D) were extracted for each control voltage by fitting the current transients with exponential functions such as in (2) and (3). Two exponential functions, representing two trap species, were found to give good fit.

As shown in Fig. 3(a), the extracted charging and discharging time constants for both positive and negative control voltages exhibit no strong voltage dependence. Therefore, τ_C and τ_D were taken as the average of the time constants extracted under different voltages. By contrast, the steady-state charge density is found to vary exponentially with the control voltage, as illustrated in Fig. 3(b). The voltage dependence of the steady-state charge density for the *Jth* trap is modeled as

$$Q^J = Q_0^J \exp(V / V_0^J) \qquad (4)$$

where V is the control voltage while Q_0 and V_0 are fitting parameters.

Using the above described approach, two sets of model parameters were extracted for positive and negative control voltages as listed in Table I. The measured and calculated transient charging and discharging currents under different control voltages are plotted in Fig. 4 showing good agreement between experimental data and theoretical calculation.

IV. MODEL VERIFICATION

The dielectric charging effect on state-of-the-art RF MEMS capacitive switches (shown in Fig. 1 and fabricated on the same wafer as the permanently down switches) was measured by applying a stress voltage on the bottom electrode of the switch for different time periods while measuring the corresponding actuation voltage. The stress voltage used in the experiment is −30 V, which is sufficient to actuate the switch. After 120 s of stress, the actuation voltage was shifted by 5 V in the positive direction indicating injection of negative charges from the bottom electrode into the dielectric.

The actuation-voltage shift due to dielectric charging can be expressed as

$$\Delta V = qhQ / \varepsilon_0 \varepsilon_r \quad (5)$$

where h is the distance between the bottom electrode and the trapped charge sheet, Q is the injected charge density predicted by (1), ε_0 is the permittivity of free space, and ε_r is relative dielectric constant of the switch dielectric.

The actuation-voltage shift for certain stress period is predicted by the charge model (1), (4) and (5) with h optimized to give the best fit between model prediction and experimental data. Fig. 5 shows the measured and modeled actuation-voltage shifts after different stress periods. Good agreement was obtained for all stress periods by using h = 90 nm, which is about one third of the dielectric thickness.

V. Discussion

Although the present model assumes that the injected charge is an equivalent sheet of charge 90 nm above the bottom electrode, the actual bottom-injected electrons most likely are distributed across the thickness of the dielectric. Since their collective effect on the actuation voltage can be approximated by a sheet charge, it greatly simplifies the model making it possible to predict the dielectric-charging effect under complicated control-voltage waveforms. In addition, tunneling and trap-to-trap hopping were not taken into account in the present simple model so that (1)-(3) are only based on the first-order carrier capture and emission dynamics. Therefore, the extracted charging and discharging time constants should not be construed as exact capture and emission times.

The current transients measured on the permanently down switches were used to predict the dielectric-charging effect in functioning switches. Although charge injection from the bottom electrode is expected to be similar in both cases, charge injection from the top electrode can be rather different due to non-ideal contact between the top electrode and the dielectric in functioning switches. For the present switches, the dielectric-charging effect is dominated by charge injection from the bottom so that any difference in charge injection from the top can be ignored. This may not be the case in other switches for which charge injection from the top is not negligible.

VI. Conclusion

Charging and discharging currents of traps in permanently down RF MEMS capacitive switches were measured. Based on the measured data, a simple charge model was extracted. The steady-state charge density was found to have an exponential dependence on the control voltage while the charging and discharging time constants were relatively independent of voltage. The extracted charge model was capable of accurately predicting charge-induced actuation-voltage shift in state-of-the-art MEMS capacitive switches.

References

[1] C. Goldsmith, J. Ehmke, A. Malczewski, B. Pillans, S. Eshelman, Z. Yao, J. Brank, and M. Eberly, "Lifetime characterization of capacitive RF MEMS switches," in *IEEE MTT-S Dig.*, 2001, pp. 227-230.

[2] X. Yuan, S. V. Cherepko, J. C. M. Hwang, C. L. Goldsmith, C. Nordquist, and C. Dyck, “Initial observation and analysis of dielectric-charging effects on RF MEMS capacitive switches,” in *IEEE MTT-S Dig.,* 2004, pp. 1943-1946.

[3] W. M. van Spengen, R. Puers, R. Mertens, and I. De Wolf, “A comprehensive model to predict the charging and reliability of capacitive RF MEMS switches,” *J. Micromechanics Microengineering*, vol. 14, pp. 514-521, Jan. 2004.

[4] H. Matsuura, M. Yoshimoto and H. Matsunami, “Discharging current transient spectroscopy for evaluating traps in insulators,” *Japanese J. Appl. Phys*., vol. 34, pp. L185-L187, Feb. 1995.